ICANS-XIV
14th Meeting of the International Collaboration on
Advanced Neutron Sources
June 14-19, 1998
Starved Rock Lodge, Utica, Illinois, USA

Discussion on the thickness optimization of the water-cooled solid target for N-arena

N.Takenaka [1], Y.Hayashida [1], R. Yasumura [1], T.Fujii [1], N.Hata [2], Y.Ogawa [2], Y.Kiyanagi [2]

1: Dept. Mechanical Engineering., Kobe Univ.,
1-1 Rokkodai, Nada, Kobe 657-8501 Japan
e-mail takenaka@mech.kobe-u.ac.jp
2: Division of Quantum Energy Engng., Graduate School of Engng., Hokkaido Univ.
Kita-13, Nishi-8, Kita-ku, Sapporo 060-8628, Japan

Abstract

Analytical results of one-dimensional (1-D) design on the thermal hydraulics of the water cooled solid target for the preliminary design of the target system in N-arena of JHF were presented. The target systems with plate disks, 60 mm x 166.6 mm in cross section with various thicknesses placed parallel with the gaps of 1.5 mm for the coolant channels were designed. The target material was tungsten. The water and the heat deposition fraction were defined and calculated for each design conditions. It was shown that the water irradiated by the beam is the least when the target thickness is designed as the intersection point in d-Q diagram is moved to the maximum heat deposition rate point by pressurizing the coolant or the heat transfer augmentation if possible.

Keywords; solid target, water cooled, thermal hydraulics, water fraction, optimization

1. Introduction

The purpose of this study is the thermal hydraulics designs of target systems in the spallation reactor to produce neutrons in N-arena of Japan Hadron Facilities.

The target systems with plate disks, 60 mm x 166.6 mm in cross section with various thicknesses placed parallel with the gaps of 1.5 mm for the coolant channels were designed. The target of N-arena is now designed to be divided into a front and a rear target. Neutrons generated mainly in the front target are moderated. The rear target is considered as the beam dump. The effective length of the front target is 300 mm.

Preliminary design of the target system to make rough sketches of the target plate designs for the N-arena were discussed. The analyses of one-dimensional (1-D) design on the thermal hydraulics of the water cooled solid target in the single coolant channel were carried out. The water fraction and the heat deposition fraction were defined and calculated to discuss the design for decreasing the water irradiated by the beam. The methods of the analyses, some results on heat transfer of the window and the target and the fractions are discussed

2. Analyses of 1-D design on the thermal hydraulics of the water cooled solid target

The heat deposition rates of a proton beam irradiated to a pure Tungsten target were calculated with a Monte-Carlo method. The beam shape was an ellipsoid 40 mm and 140 mm in diameters and the intensity distribution was assumed to be parabolic. The target was a block 60 mm x 166.7 mm in rectangular cross section and 500 mm in depth. The distributions of the heat deposition rates along the beam line averaged in the whole cross section (axis) and in a cylinder 20 mm in diameter at the center of the cross section (center axis) were obtained. The both calculated results were fitted with an empirical equation are shown in Fig.1, respectively. The heat deposition rates in the beam window made from stainless steel 304 and Inconnel 600 were also calculated in the same methods.

The wall and the maximum temperatures are highest at the center of the target plate. To estimate the highest temperatures in a target plate by 1-D equations, they were calculated with an assumption that the heat deposition rate over the target is uniform at the value obtained by center axis shown in Fig.1(b). The predicted temperatures were low, i.e., had some safety margin comparing with those by the 3-D results.

The thermal hydraulics conditions from the safety considerations for the water cooled target plate are as follows:

(a) The heat flux at the target surface is below the critical heat flux.
(b) The temperature at the target surface is below the saturation temperature of the water to avoid boiling.
(c) The maximum temperature in the target is below a certain temperature much lower than the melting point of the target material.
(d) The thermal stress in the target is below a certain value smaller than the yield stress or the stress which causes the deformation of the coolant channel.
(e) Water irradiated by the proton beam, i.e., water fraction of the target is as little as possible.

The conditions for the beam window are the same as (a)-(d).

The conditions of (a) and (b) are based on the heat convection in the coolant and those of (c) and (d) on the heat conduction in the target. The equations used for these conditions are summarized in Table 1. The configurations of the target and the coolant channel are shown in Fig.2. The coolant temperature in the channel can be calculated by the enthalpy conservation.

The wall surface and the maximum temperatures are mainly discussed in this report. Since the critical heat fluxes for the coolant conditions are estimate to be much higher than the heat fluxes estimated by the conditions (b) and (c), they are not discussed in this report. The details of the thermal stress should be discussed for the 3-D geometry and 1-D calculations on the thermal stress were made for the estimation in this paper.

The thickness of the target plate which allow the conditions from (a)-(d) can be calculated at a given heat generation rate. The thickness of the target which agree with the conditions (a) and (b) is proportional to the heat deposition rate while that with the conditions (c) and (d) proportional to its square. Therefore, the relation between the heat deposition rate and the thickness of the target plate is illustrated by a d-Q diagram as shown in Fig.3. The minimum target thickness d_{min} is determined by the maximum heat deposition rate Q_{max} as shown in the figure. It can be seen that the target thickness is determined by the conditions (a) or (b) in high heat deposition conditions and by the conditions (c) or (d) in low heat deposition conditions. The former conditions are based on the heat convection where the target thickness is determined by the heat transfer at the wall surface without the effects of the target material. The limit of the wall temperature can be changed by the system pressure and the wall temperature can be decreased when the heat transfer augmentation is carried out. Two or three times heat transfer augmentation may be possible if the target wall surface was machined to certain shape. The latter are based on the heat conduction in the target material. The

limit of the maximum temperature was determined by the material strength and the target shape and was not much changed by the thermal hydraulic condition.

For the discussion on the condition (e) water fraction f_w and heat deposition fraction f_Q were defined. The target of N-arena is divided into front and rear target. Neutrons generated mainly in the front target are moderated. The rear target is considered as the beam dump. The effective length of the front target L_{eff} is 300 mm in the present calculation.

These fractions are defined in the front target as

$$f_w = n\,\delta / L_{eff}\,, \quad f_Q = \Sigma Q_i d_i / \int Q(z)dz$$

where suffix i means the i-th target plate counted from the beam side and n is the number of the target plates in the effective length.

2-1. Calculated results on the target design

Examples of the calculated results for the target at the position where the heat deposition rate is the highest for the proton beam power 0.6 and 1.2 MW in N-arena. The target material was tungsten and the width of the coolant channel was fixed at 1.5 mm.

The temperatures at the target wall surface and the maximum temperatures of the target at the center are shown in Figs.4 and 5 against the velocity for the target thickness from 3 to 10 mm. C in Table 1 is a parameter to estimate the entrance region. C=4 is the most realistic for the target assembly. C=0 is the most safety design and was used in this calculation.

The wall surface and the maximum temperatures of the beam window are shown in Figs.5 and 6 for 3 and 5 mm thick stainless steel 304 and Inconnel 600, respectively. Since the beam window was cooled at one side by water and the other side was adiabatic, the maximum temperature is at the beam side surface.

The thickness of the target is determined by the heat convection or the heat conduction depending on the heat deposition rate as described before. The target thickness distributions along the beam line were determined for the heat deposition rate distribution shown in Fig.1(b). The width of the coolant channel and the coolant inlet temperature were fixed 1.5 mm and 30 C, respectively.

The distributions of the heat deposition rate, the target thickness, the heat flux, the wall and the maximum temperatures and the maximum thermal stress are shown in Fig.8 where W_p, u_{ch}, T_{max}* and T_w* are the beam power, the coolant velocity in the channel and the limit of the maximum and wall surface temperatures for the design, respectively. The thicknesses of the target were calculated based on the heat convection near the beam window where the wall temperature was kept to the designed value and the heat flux was also constant. After the cross point shown in the d-Q diagram in Fig.3, they were calculated based on the heat conduction where the maximum temperature was kept to the designed value and the thermal stress was also constant. The designed values of the wall surface and the maximum temperature, T_w* and T_{max}*, should be determined by the pressure and the strength of the target material, respectively.

2.2 Water and heat deposition fractions

The water and the heat deposition fractions as defined above, f_w and f_Q are shown by the lines against the limit of the wall temperature T_w* for T_{max}* of 200, 250 and 300 C in Figs.9 and 10 where the minimum target plate thicknesses are also plotted by the symbols. With increasing T_w*, f_w decreases, f_Q and d_{min} increase at first, and then they keep constant values after certain values of

T_w*. The conditions on d-Q diagram at the points (a)-(c) in this figure are shown and the certain point is at where the maximum heat deposition rate is at the value of the intersection points of two lines in d-Q diagram. It can be seen that the water irradiated by the beam is the least when T_w* can increase up to the value at the point (b) with pressurizing the coolant. Or it can be seen further increase of T_w* after the point (b) is meaningless to decrease the water fraction and there is the limit to decrease the water fraction by the pressurization of the coolant.

The effects of the heat transfer augmentation rate, h_A/h, on the fractions are shown in Figs. 11 and 12, where h_A and h means the augmented and the normal heat transfer coefficient, respectively. More augmented is the heat transfer, f_w decreases and f_Q increases but the rates of the increase and decrease become very small after certain values of T_w*. The reason is just the same as above. So it can also be seen that there is a limit to decrease the water fraction effectively by the heat transfer augmentation.

It was shown that the water irradiated by the beam could be decreased by the pressurization or the heat transfer augmentation but there were limits to decrease the water fraction. The limits is determined when the target thickness is designed as the intersection point in d-Q diagram is moved to the maximum heat deposition rate point, i.e., the target thicknesses are determined in the heat conduction region.

3. Conclusions

Analytical results with 1-D model are presented as the preliminary designs for the thermal hydraulic of the solid target for N-arena in JHF. Water and heat deposition fractions were defined and the design conditions to decrease the water irradiated by the beam were discussed.

The water irradiated by the beam could be decreased by the pressurization or the heat transfer augmentation but there were limits to decrease the water fraction. The limits is determined when the target thickness is designed as the intersection point in d-Q diagram is moved to the maximum heat deposition rate point.

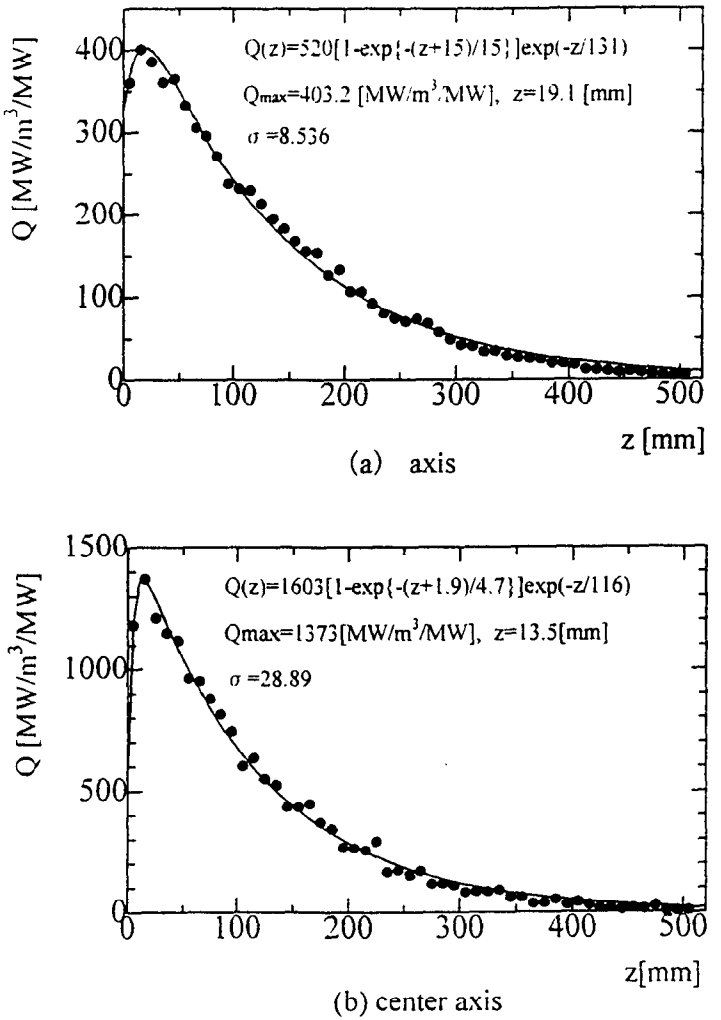

Fig.1 Heat deposition rate in target

Equations for One-dimensional Design

Critical Heat Flux and Wall Temperature

$$q = \frac{Qd}{2} = h(T_w - T_L)$$

$$Nu = 0.023 Re^{0.8} Pr^{0.4}\left(1 + \frac{C}{z/D}\right), \quad Nu = \frac{hD}{\lambda_L}, \quad Re = \frac{uD}{\nu_L}$$

$$q < q_{crit}, \quad T_w < T_{sat}$$

Maximum Temperature and Wall Stress

$$T_{max} - T_w = \frac{1}{8\lambda_s} Qd^2$$

$$T_{max} << T_{m.p.}$$

$$\tau_s = \frac{\alpha E}{12\lambda_s(1-\nu)} Qd^2 = \frac{2\alpha E}{3(1-\nu)}(T_{max} - T_w)$$

$$\tau_s < \tau_{max}$$

Design Results

T_w, q_{crit} ; $Qd <$ Designed Value

T_{max}, τ_{max} ; $Qd^2 <$ Designed Value

Table 1. Equations used for the calculation

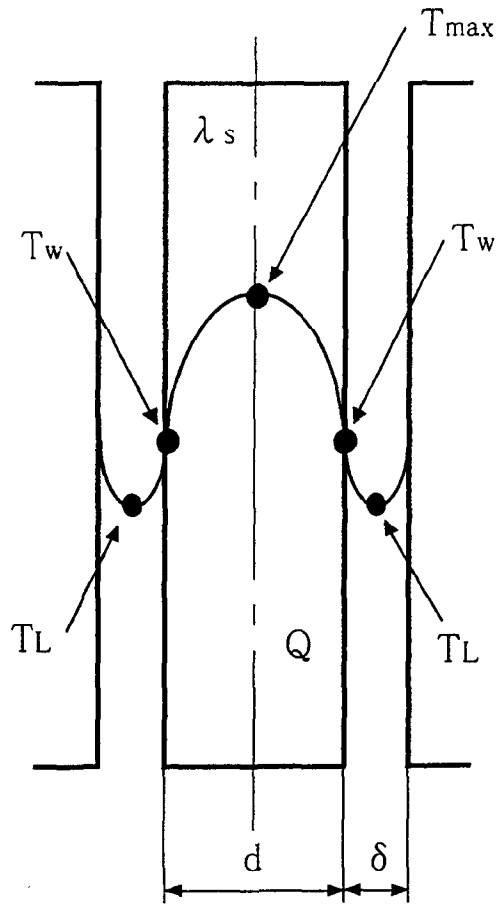

Q: heat deposition rate [W/m^3]
T_w: target wall sarface temperature [℃]
T_{max}: target maxmum temperature at center [℃]
T_L: coolant temperature [℃]
d: target thikness [m]
δ : coolant channel width [m]
λ_s: thermal conductivity of target material [W/mK]

Fig.2 Target and coolant channel

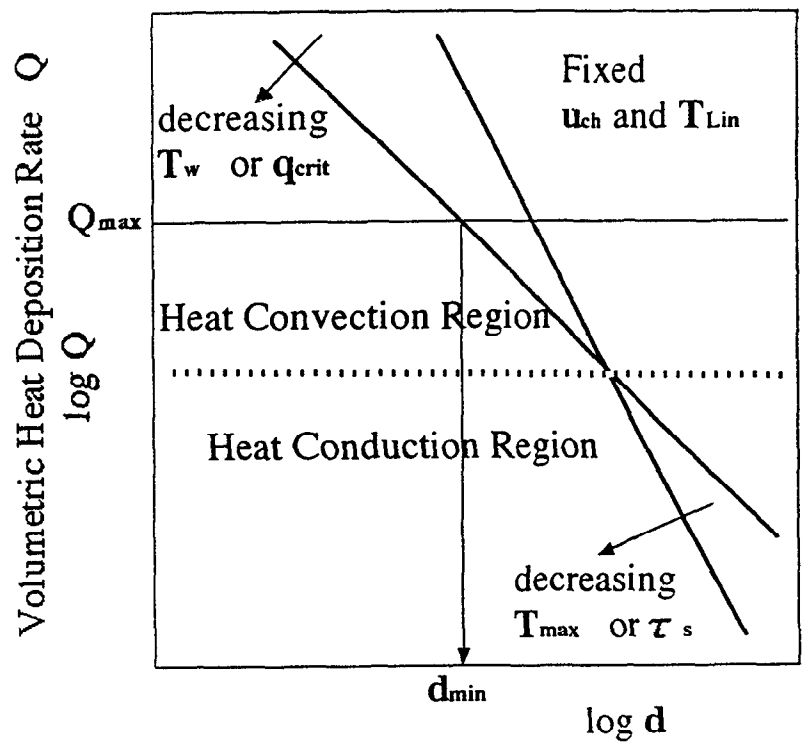

Fig.3 Relationships of thickness of target d and volumetric heat generation rate Q, d-Q diagram

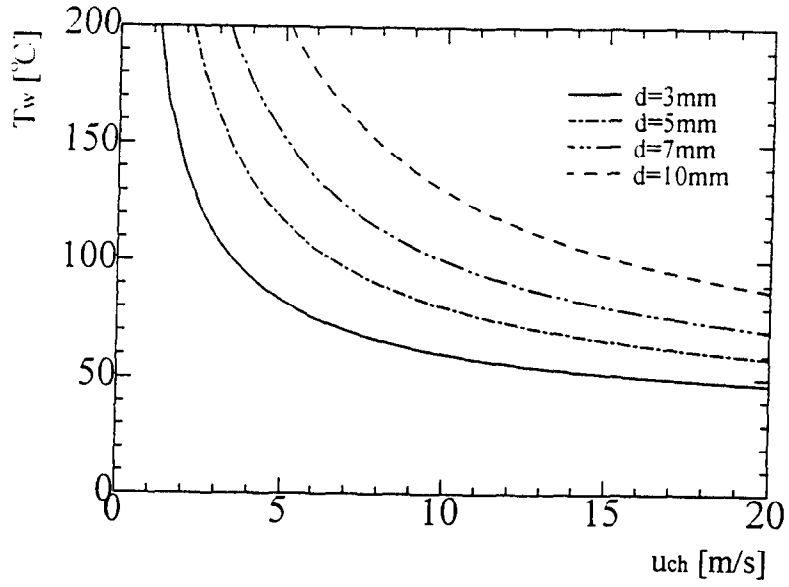

(a) WP=0.6MW

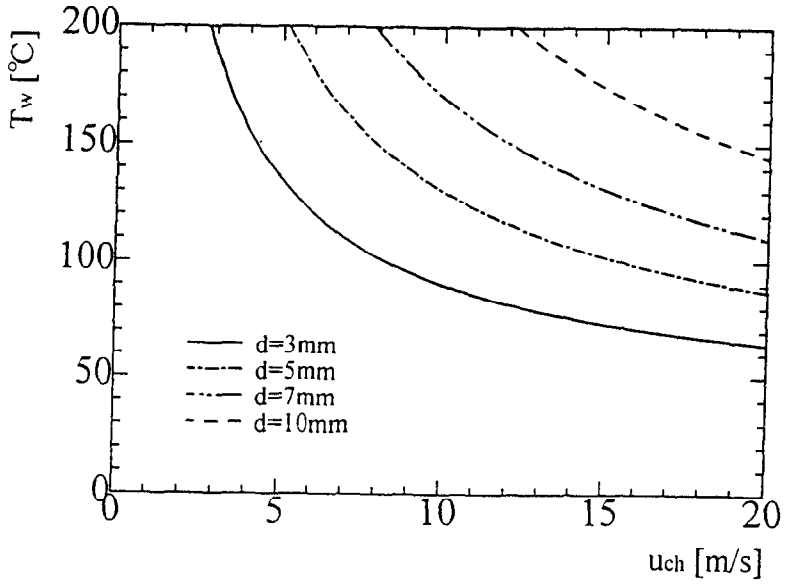

(b) WP=1.2MW

Fig.4 Wall surface temperature of target

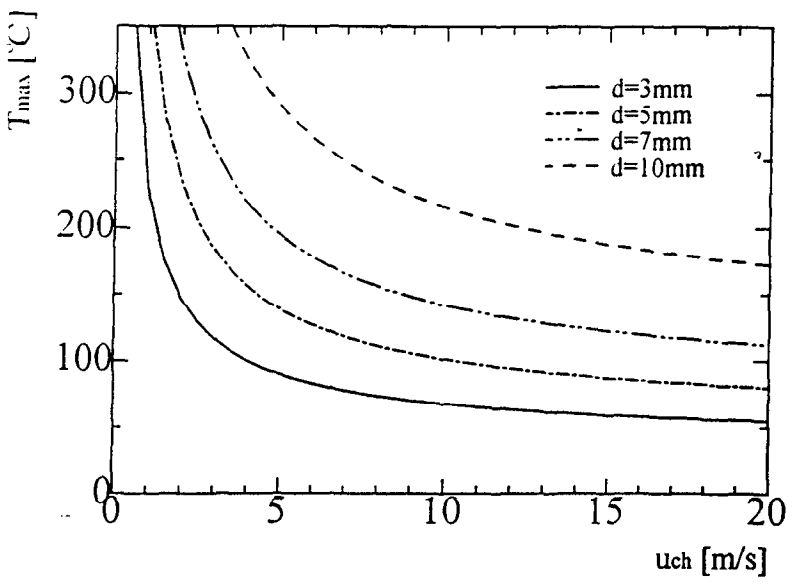

(a) WP=0.6MW

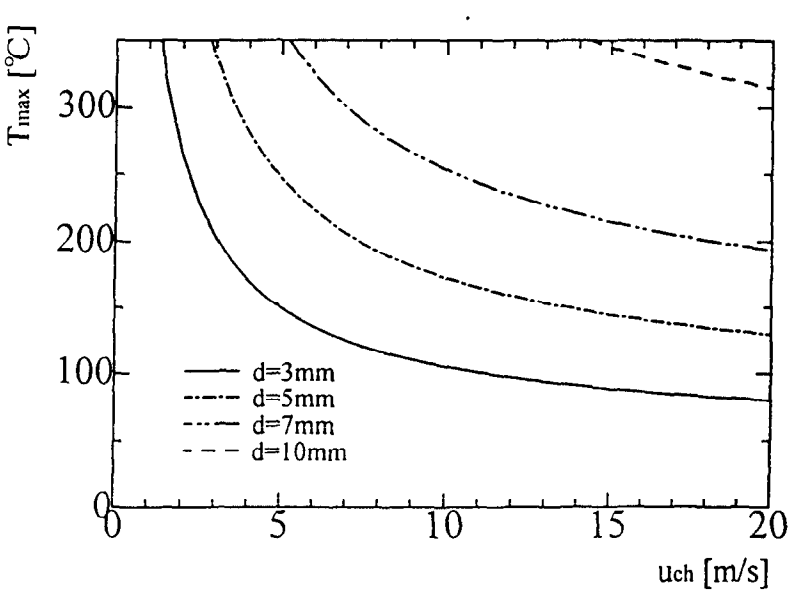

(b) WP=1.2MW

Fig.5 Maximum temperature of target

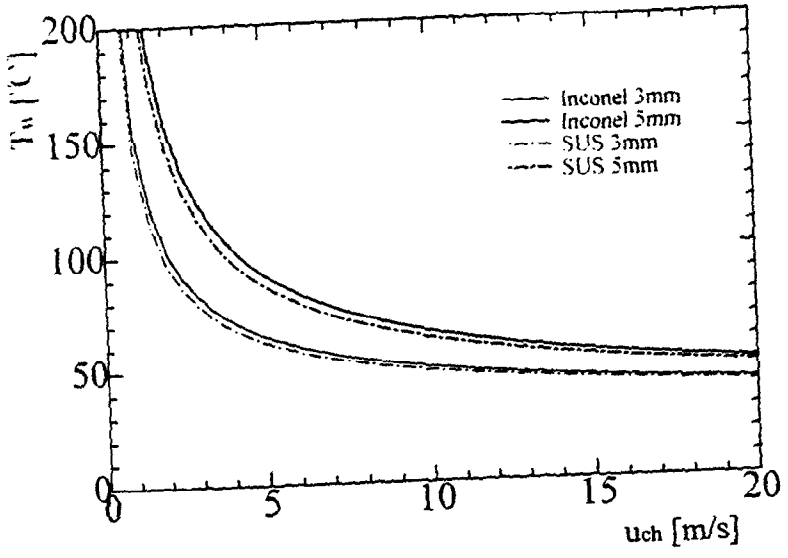

W_p=0.6MW, C=0, T_{Lin}=30℃, δ =1.5mm, L=167mm

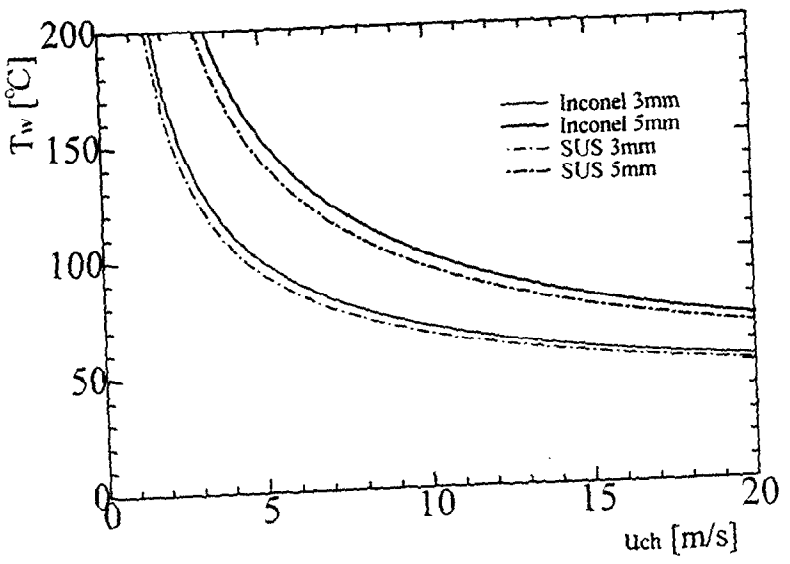

W_p=1.2MW, C=0, T_{Lin}=30℃, δ =1.5mm, L=167mm

Fig.6 Wall surface temperature of window

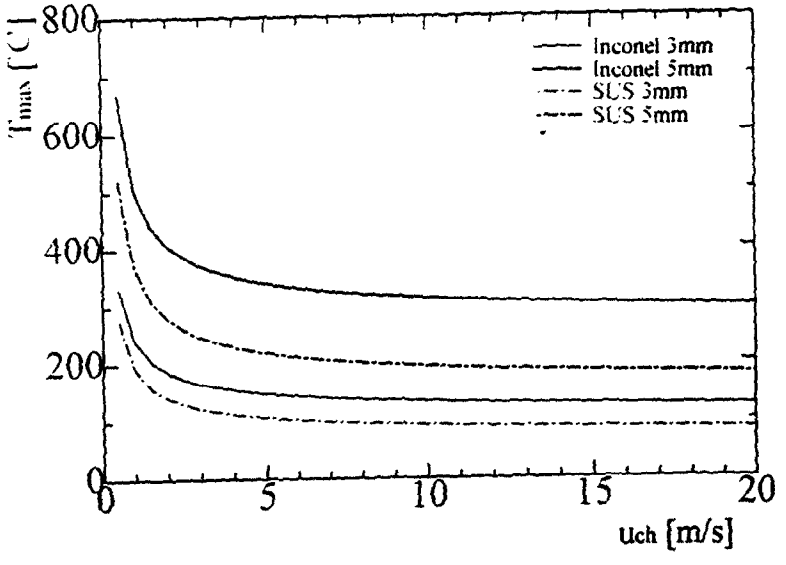

W_p=0.6MW, C=0, T_{Lin}=30℃, δ =1.5mm, L=167mm

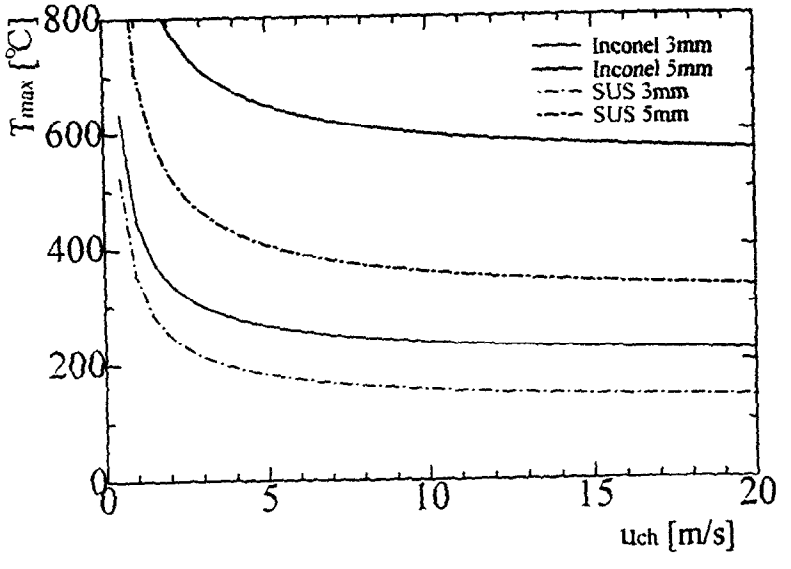

W_p=1.2MW, C=0, T_{Lin}=30℃, δ =1.5mm, L=167mm

Fig.7 Maximum temperature of window

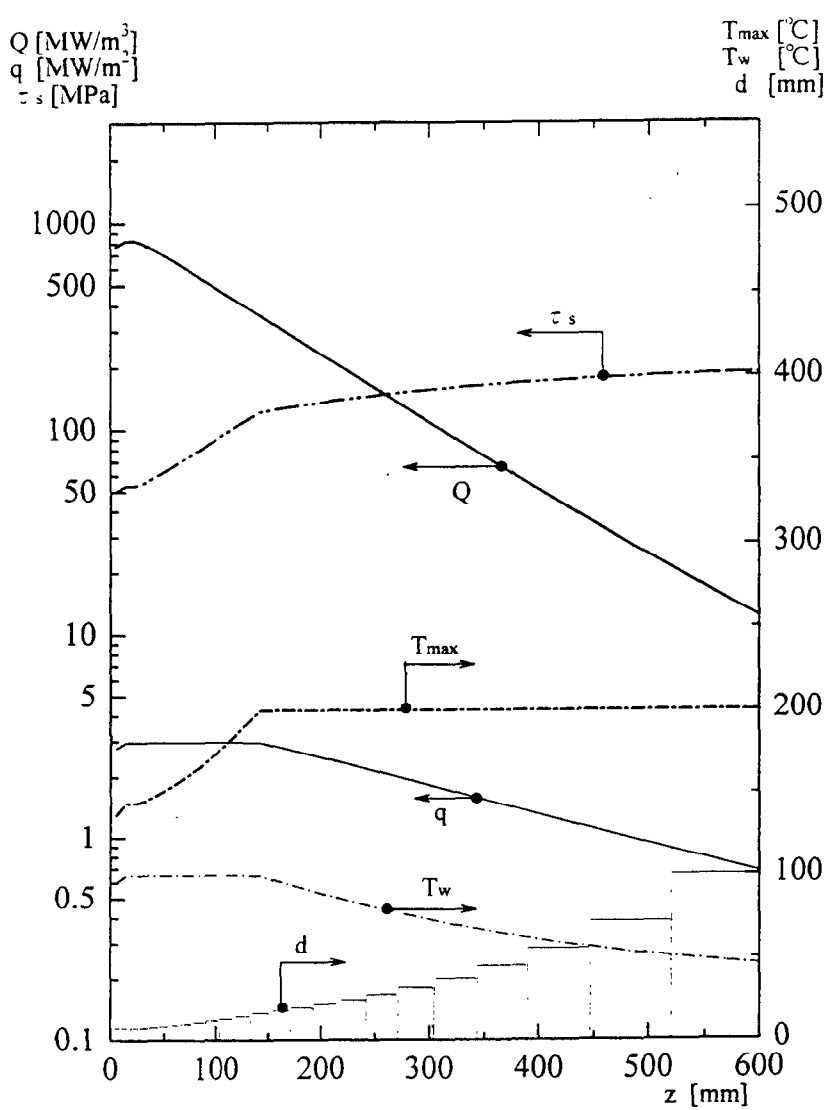

Wp=0.6MW, uch=10m/s, Tmax*=200℃, Tw*=100℃

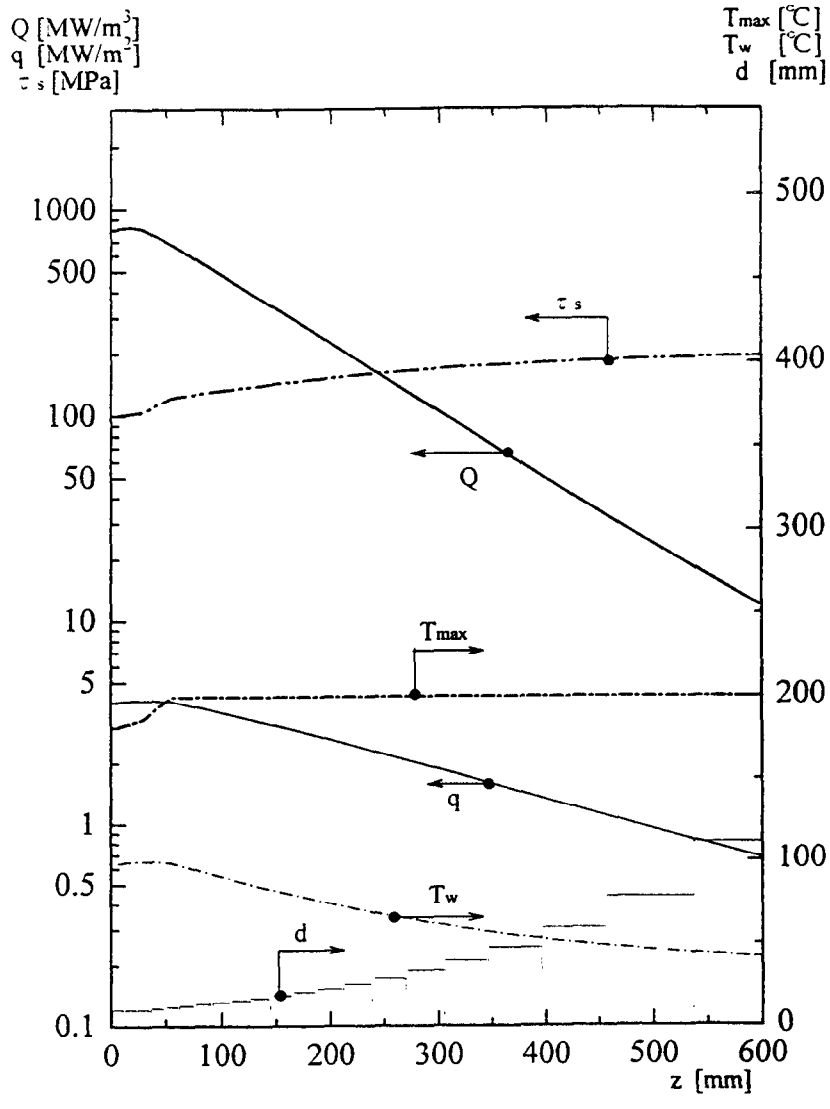

Wp=0.6MW, uch=15m/s, Tmax*=200℃, Tw*=100℃

Fig.8 Target design results

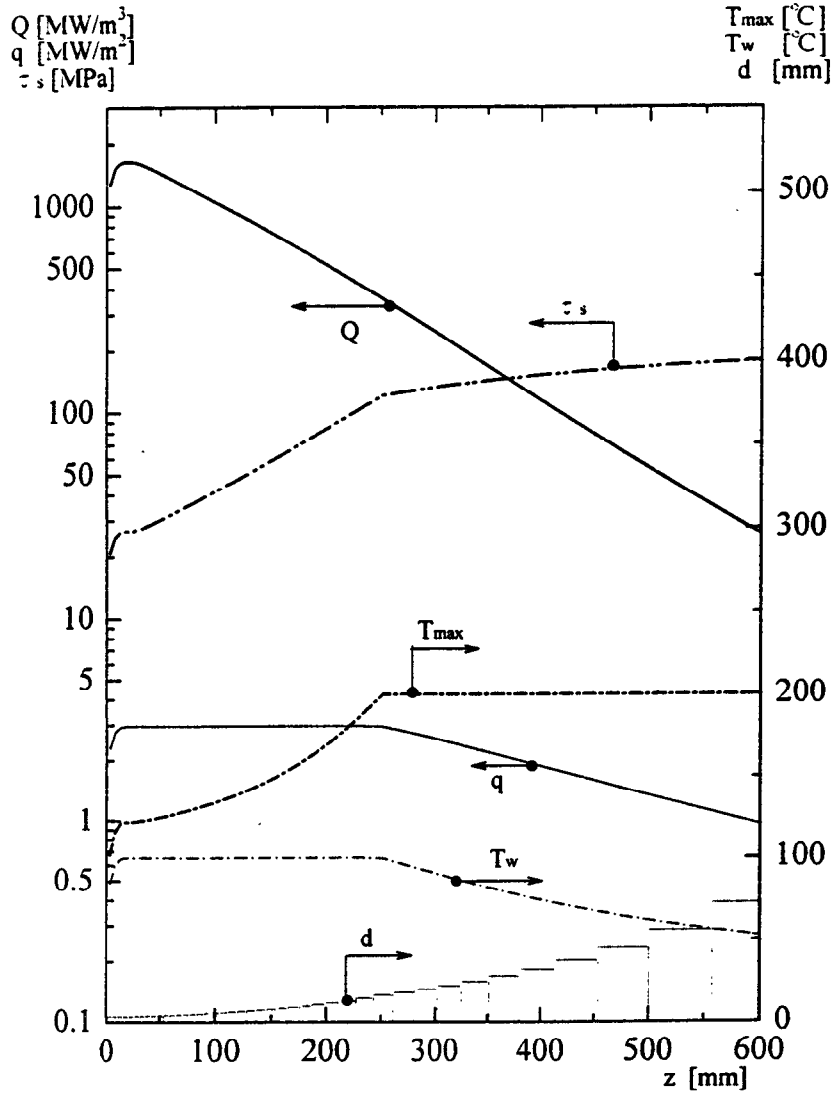

W_p=1.2MW, u_{ch}=10m/s, T_{max}*=200℃, T_w*=100℃

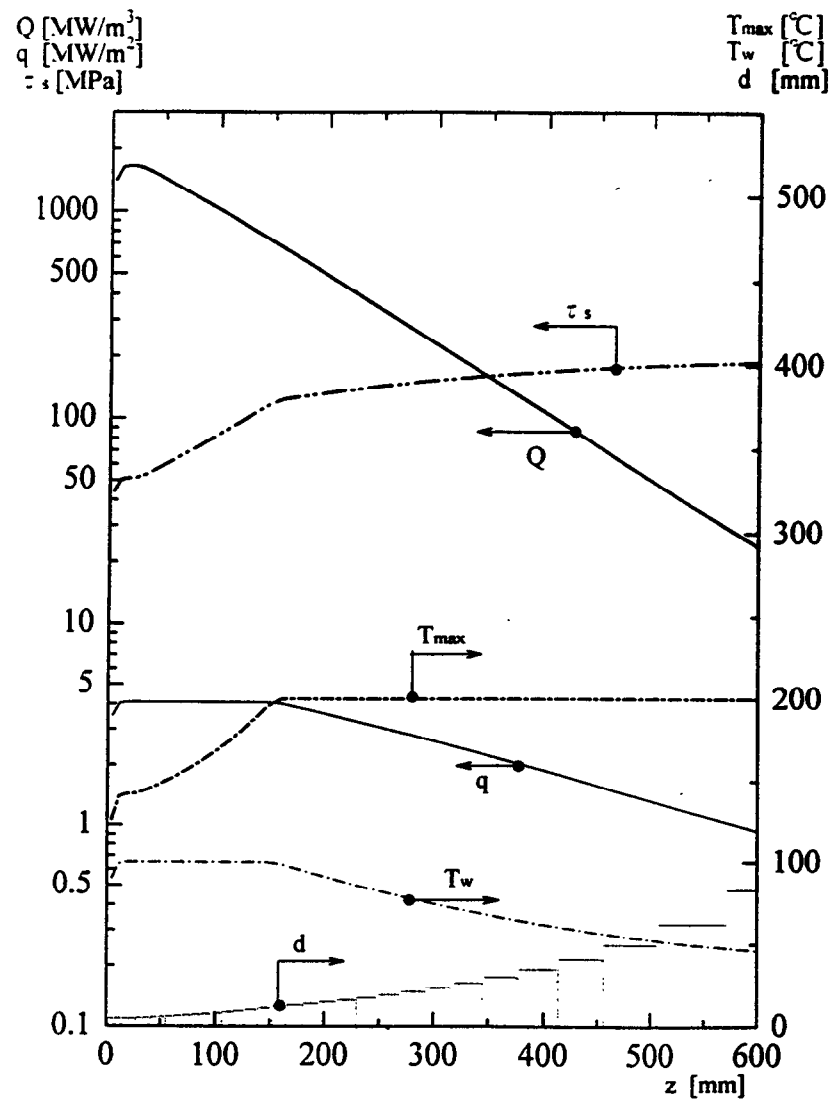

W_p=1.2MW, u_{ch}=15m/s, T_{max}*=200℃, T_w*=100℃

Fig.8 Target design results

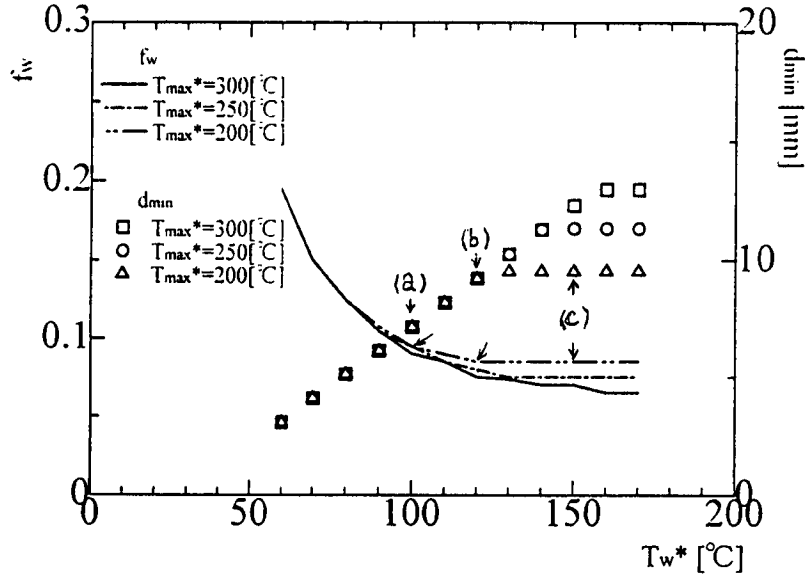

Wp=0.6MW, uch=10m/s, C=0, TL=30℃, δ=1.5mm, L=167mm

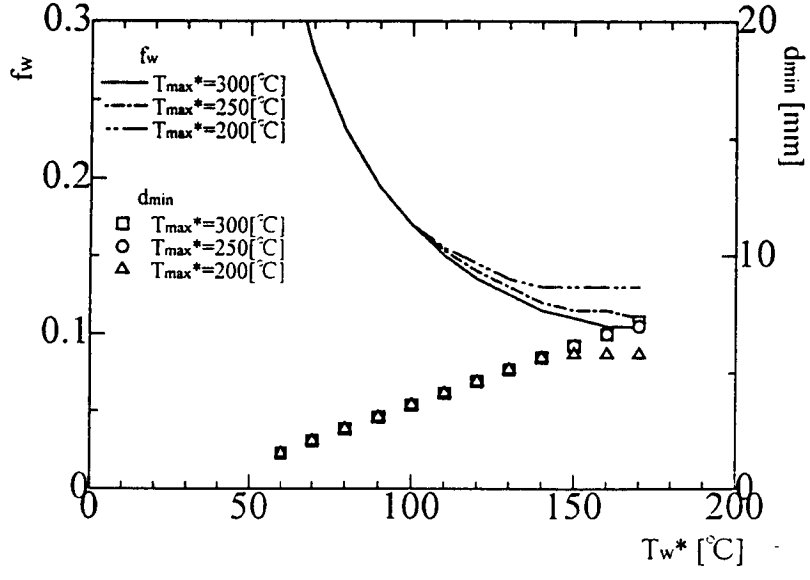

Wp=1.2MW, uch=10m/s, C=0, TL=30℃, δ=1.5mm, L=167mm

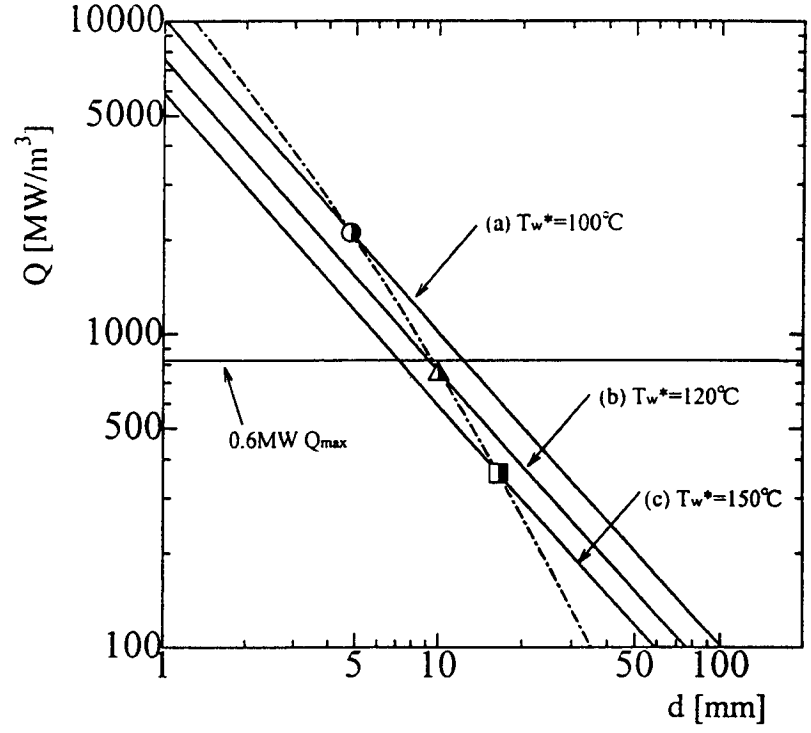

Tmax*=200℃, TL=30℃, uch=10m/s, C=0, δ=1.5mm, L=167mm

Fig.9 Water fraction f_W and d-Q diagram for wall temperature limit T_W*

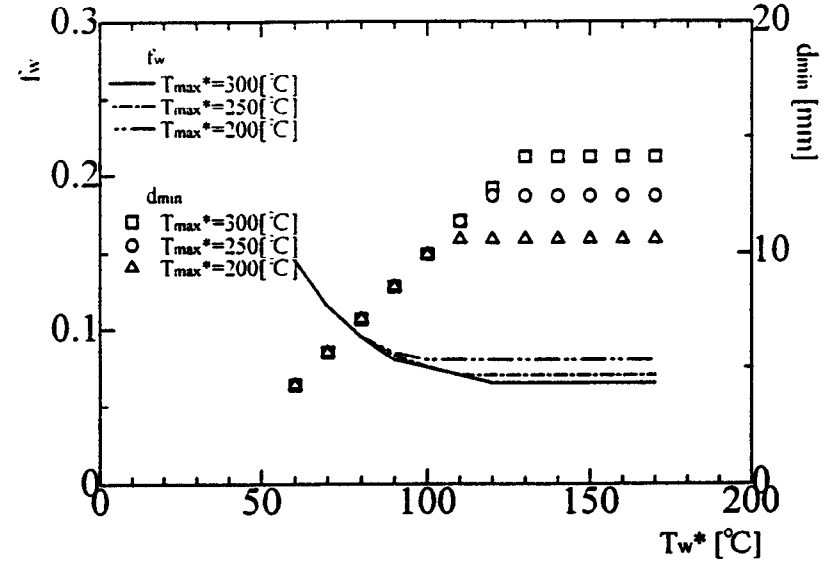

W_p=0.6MW, u_{ch}=15m/s, C=0, T_L=30℃, δ =1.5mm, L=167mm

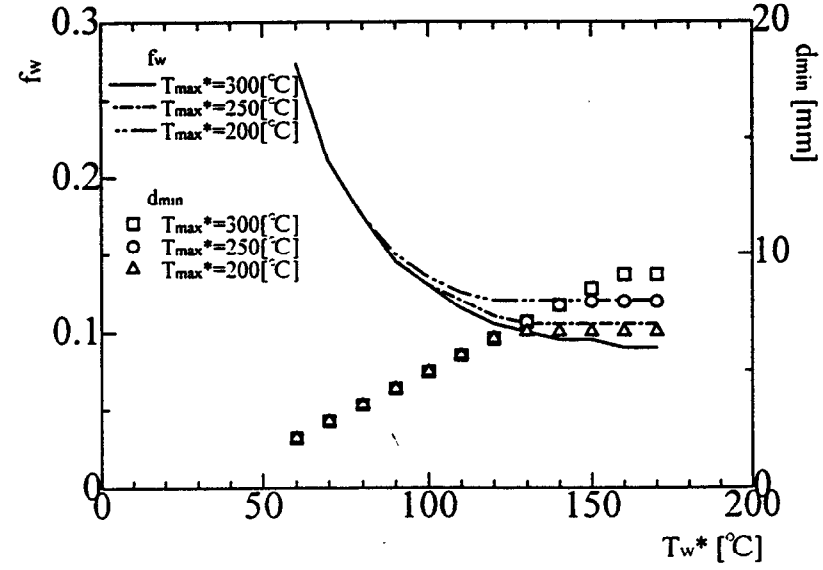

W_p=1.2MW, u_{ch}=15m/s, C=0, T_L=30℃, δ =1.5mm, L=167mm

Fig.9 Water fraction f_W and d-Q diagram for wall temperature limit T_W*

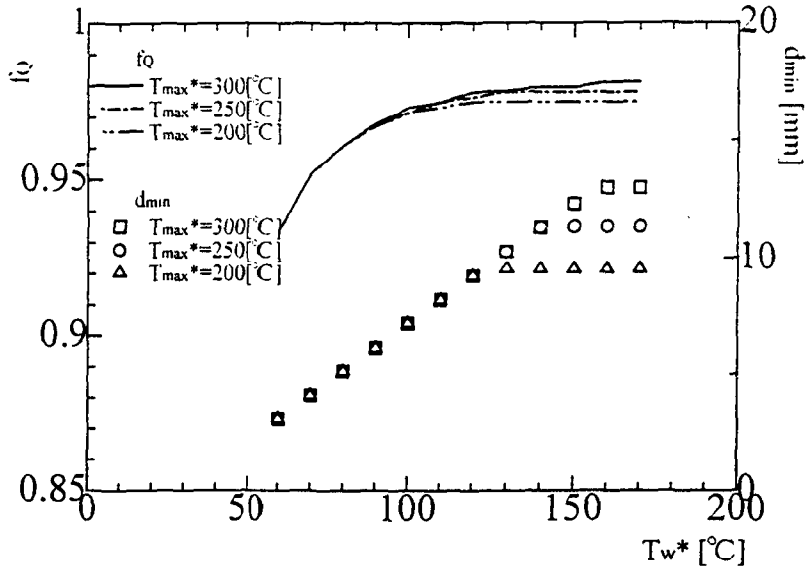

Wp=0.6MW, uch=10m/s, C=0, TL=30℃, δ =1.5mm, L=167mm

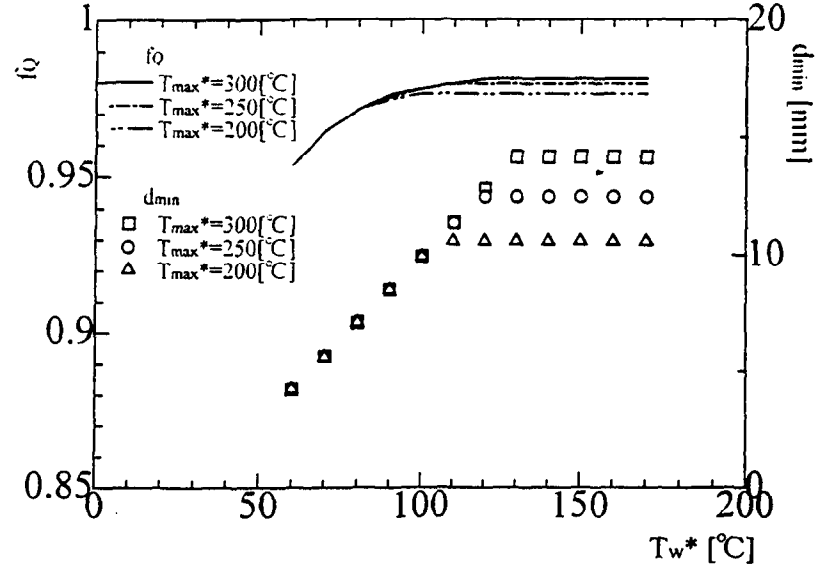

Wp=0.6MW, uch=15m/s, C=0, TL=30℃, δ =1.5mm, L=167mm

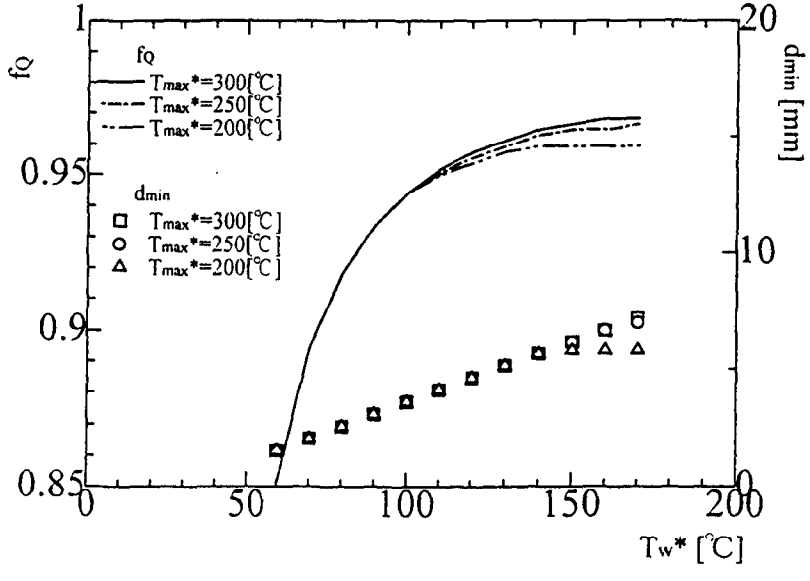

Wp=1.2MW, uch=10m/s, C=0, TL=30℃, δ =1.5mm, L=167mm

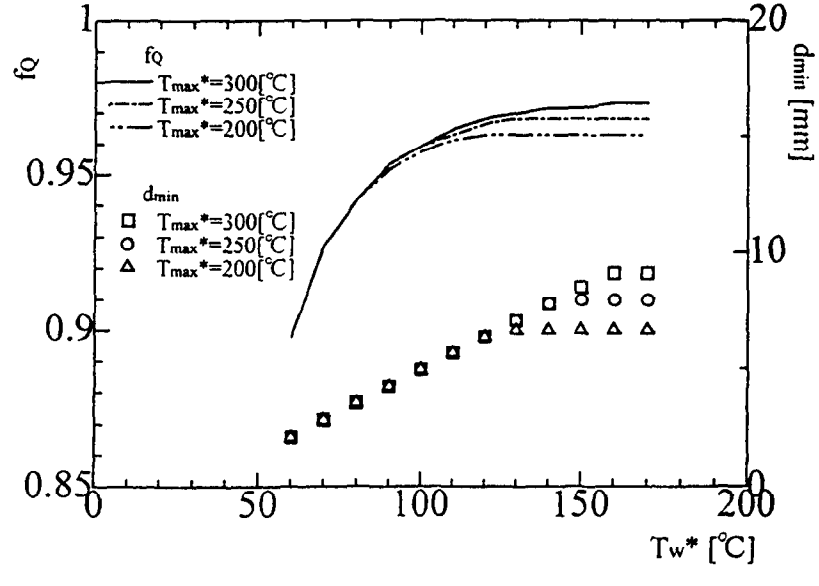

Wp=1.2MW, uch=15m/s, C=0, TL=30℃, δ =1.5mm, L=167mm

Fig.10 Heat deposition rate fraction for wall temperature limit T_w*

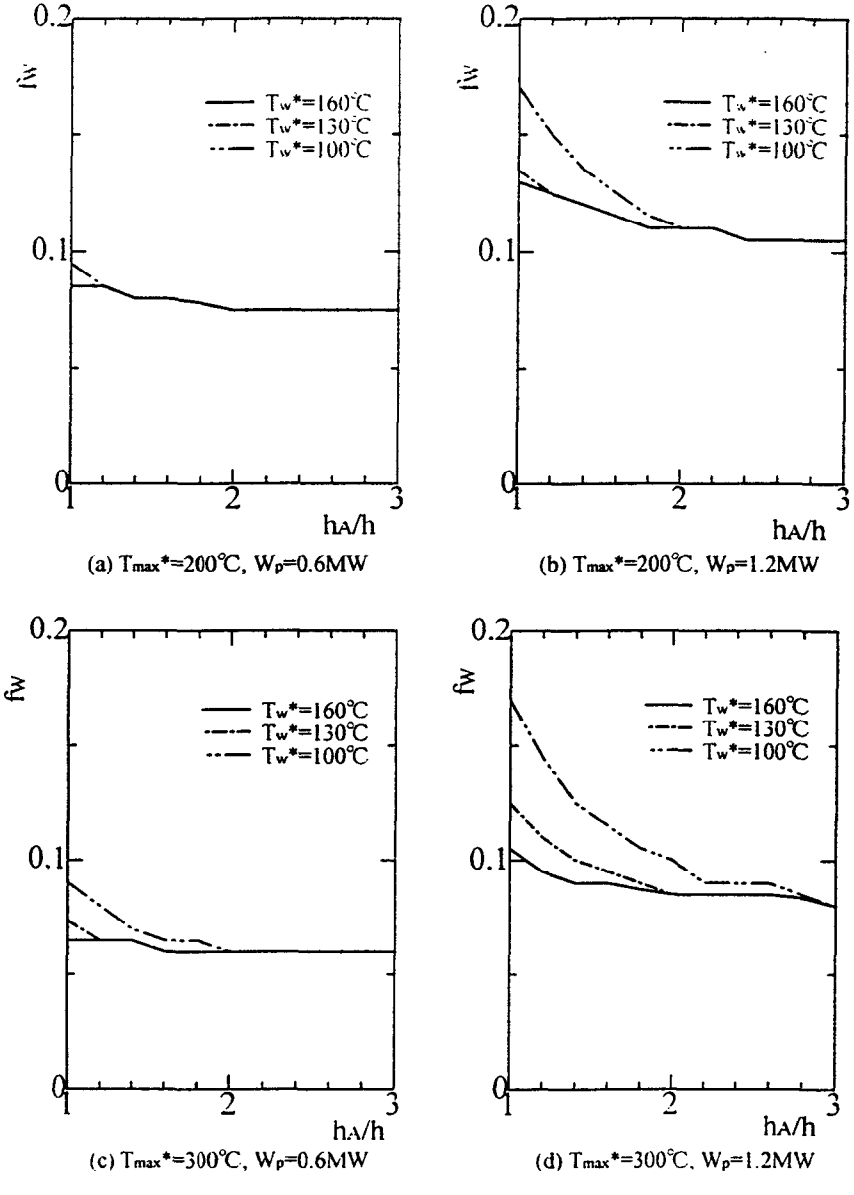

Fig.11 Water fraction f_W for heat transfer augementation rate h_A/h

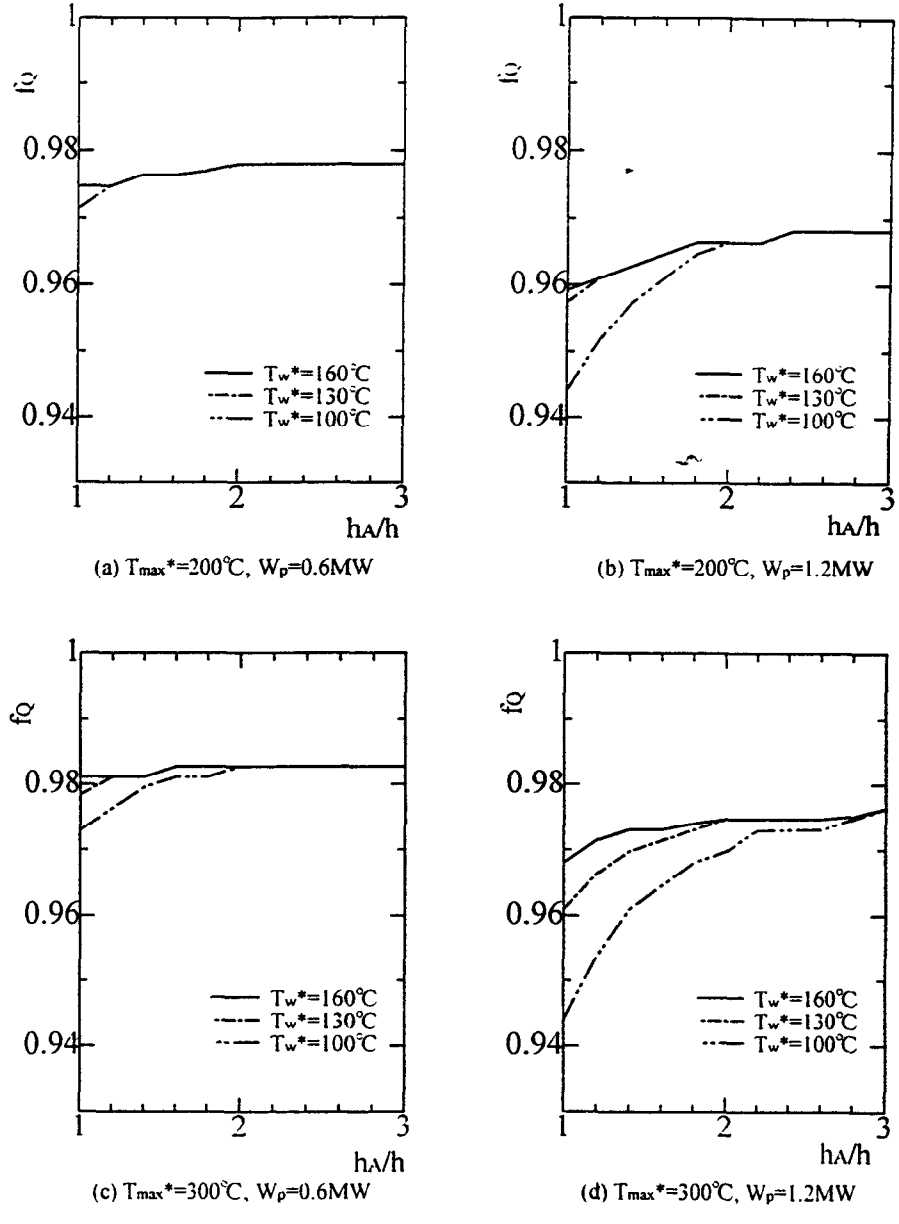

Fig.12 Heat deposition rate fraction f_Q for heat transfer augementation rate h_A/h